High-power high-repetition-rate subpicosecond monolithic Yb:KGW laser with self-mode locking

W. Z. Zhuang, M. T. Chang, H. C. Liang, and Y. F. Chen*

Department of Electrophysics, National Chiao Tung University, Hsinchu 30010, Taiwan
**Corresponding author: yfchen@cc.nctu.edu.tw*

Received May 22, 2013; revised June 21, 2013; accepted June 24, 2013;
posted June 25, 2013 (Doc. ID 190970); published July 15, 2013

We report on a high-power subpicosecond monolithic self-mode-locked Yb:KGW laser with the pulse repetition rate up to several tens of gigahertz. Experimental results reveal that not only the repetition rate but also the pulse width depend on the length of the laser crystal. Using a coated Yb:KGW crystal with a length of 3.36 mm, mode-locked pulses with pulse duration of 850 fs at the repetition rate of 22.4 GHz have been achieved. With an incident pump power of 10.5 W, an average output power of 3.6 W was achieved which corresponds to the optical conversion efficiency of 34.3%.

OCIS codes: (140.3480) Lasers, diode-pumped; (140.4050) Mode-locked lasers; (140.5680) Rare earth and transition metal solid-state lasers.
http://dx.doi.org/10.1364/OL.38.002596

High-power light sources with pulse repetition rates up to gigahertz (GHz) and pulse durations in the picosecond and sub-picosecond (sub-ps) regime have attracted intensive attention for applications, such as optical frequency comb spectroscopy [1], high capacity optical networks [2], laser cooling [3], optical clocking [4], and arbitrary waveform generation [5]. Mode-locked, diode-pumped solid-state lasers are desirable methods for combining advantages of compactness, low cost, high efficiency together with high-repetition-rate operation.

Among rare-earth-doped crystals used in diode-pumped laser systems, Yb-doped laser crystals have been identified to be promising materials for efficiently mode-locked operations [6–10] owing to the small quantum defect and the exclusion of parasitic effects, such as excited state absorption and up-conversion. Compared with other Yb-doped laser crystals, the Yb:KGd$(WO_4)_2$ (Yb:KGW) crystal is a superior candidate for efficiently generating sub-ps pulses with high repetition rates due to its broad gain bandwidth (24 nm), high absorption cross section (5.3×10^{-20} cm^2), and large emission cross section (2.8×10^{-20} cm^2). Recently, a passively mode-locked Yb:KGW laser with the repetition rate of 4.8 GHz and the pulse duration of 396 fs has been demonstrated by employing a semiconductor saturable absorber mirror [9]. On the other hand, the diode-pumping scheme has been successfully used to achieve efficient self-mode-locked operations in Yb-doped [6–8] and Nd-doped [11,12] crystal lasers. Here, the self-mode locking (SML) means that no additional active or passive mode-locking elements (such as saturable absorbers) are used in the laser cavity except for the gain medium. So far, the origin of the SML is conjectured to result from the combined effects of the Kerr-lensing and thermal lensing together with gain aperturing [6,7,11,12]. The advantage of a simple linear cavity in the SML operation opens up the feasibility of achieving an ultra-high repetition rate. Furthermore, previous investigations reveal that the laser host with a high nonlinear refractive index is of use in achieving fairly stable SML operations [7,11,12]. Even though the Yb:KGW crystal possesses a considerable nonlinear refractive index (20×10^{-16} cm^2/W) [13], to the best of our knowledge, there is no report on the SML operation of the Yb:KGW crystal until now.

In this Letter, we demonstrate the use of the Yb:KGW crystal as a monolithic cavity to achieve an efficient SML operation with the repetition rate up to several tens of GHz. Different crystal lengths are employed to obtain various pulse repetition rates and pulse durations. With a crystal length of 3.36 mm, the experimental results for the pulse repetition rate and the pulse duration are 22.4 GHz and 850 fs, respectively. At an incident pump power of 10.5 W, an average output power of 3.6 W is attained, corresponding to an optical conversion efficiency of 34.3%.

Figure 1 shows the experimental setup for the monolithic SML operation. The gain media were Yb:KGW crystals cut along the ng-axis and doped with 5 at. % Yb^{3+} doping concentration for all different crystal lengths. The crystal length included 2.25, 3.36, 6.47, and 10.26 mm. We did not use Yb:KGW crystal with shorter crystal length due to the insufficient pump absorption with the given doping concentration. One of the end facet of the crystal was coated for high reflection (HR, $R > 99.8\%$) centered at 1065 nm with total spectral bandwidth of 70 nm (1030–1100 nm) and high transmission (HT, $T > 95\%$) at 980 nm to serve as the front mirror. The rear facet was coated for high reflection (HR, $R > 99\%$) at 980 nm to increase the absorption efficiency of the pump power and was coated for partial reflection (PR, $R \approx 96\%$) centered at 1050 nm with total spectral

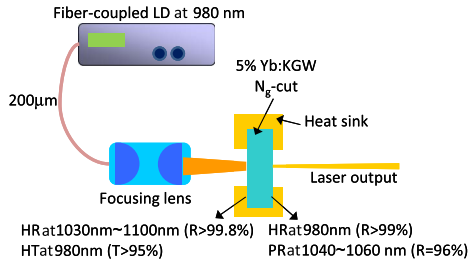

Fig. 1. Schematic diagram of the mode-locked Yb:KGW laser experimental setup.

bandwidth of 20 nm (1040–1060 nm) to serve as the output coupler.

The Yb:KGW crystal was wrapped with indium foil and mounted within a water-cooled copper heat sink at 8°C to ensure stable laser output. The pumping source was a 980 nm fiber-coupled laser diode with a core diameter of 200 μm and a numerical aperture of 0.2. A lens with a focal length of 25 mm was used to focus the pump beam into the laser crystal. The overall coupling efficiency was nearly 90%. The pump spot radius was approximately 220 μm.

Figure 2 depicts the average output power versus the incident pump power with different crystal lengths. The laser pump thresholds were 2.7, 5.0, and 6.6 W for the crystal lengths of 3.36, 6.47, and 10.26 mm, respectively. It can be seen that under the pump power of 10.5 W, the average output powers were 3.6, 2.1, and 1.3 W for the crystal lengths of 3.36, 6.47, and 10.26 mm, respectively. The lasing performance obtained with the crystal length of 2.25 mm was found to be significantly inferior to the result obtained with the crystal length of 3.36 mm due to the insufficient absorption and more serious thermal effects because there was less contacted surface between the crystal and the copper heat sink for heat extraction. Besides, the strength of the saturable absorption effect for Kerr-lensing is also reduced with the shortest crystal length of 2.25 mm which is an obstacle to attain stable SML operation. In other words, the optimal crystal length was approximately 3–4 mm. With a crystal length of 3.36 mm, the optical-to-optical conversion efficiency and the slope efficiency were measured to be 34.3% and 46.2%, respectively. The deterioration of the optical conversion efficiency for the cases with crystal lengths of 6.47 and 10.26 mm was mainly attributed to the rise of the reabsorption and the scattering losses in the gain medium.

The first- and second-order autocorrelations were exploited to analyze the temporal behavior of the laser output. The first-order autocorrelation trace is attained with a Michelson interferometer (Advantest Q8347) with a resolution of 0.003 nm that is also able to perform optical spectral analysis by Fourier transforming the first-order field autocorrelation. The second-order autocorrelation trace is obtained with a commercial autocorrelator (APE pulse check, Angewandte Physik & Elektronik GmbH). The mode-locked pulses were detected by a high-speed InGaAs photodetector (Electro-optics Technology, Inc. ET-3500 with rise time of 35 ps) whose output signal was connected to a RF spectrum analyzer (Advantest R3265A) with a bandwidth of 8 GHz and a digital oscilloscope (Agilent DSO 80000) with 10 GHz electrical bandwidth and sampling interval of 25 ps. We observed that once the pump power reached the lasing threshold, the system instantaneously stepped into the stable mode-locked regime and kept stable over day-long operation. As a consequence, the laser contained no hysteresis phenomena and was stable for all the varied pump power range. Figure 3(a) shows the experimental result of first-order autocorrelation trace at the maximum output power of 3.6 W with the crystal length of 3.36 mm. The pulse repetition rate was measured to be 22.4 GHz which corresponds exactly to the free spectral range of the optical cavity length. With the refractive index of 1.986, the optical cavity lengths for the Yb:KGW crystals with crystal lengths of 3.36, 6.47, and 10.26 mm were approximately 6.69, 12.85, and 20.38 mm, respectively. Figure 3(b) depicts the optical spectrum derived from the experimental first-order autocorrelation trace shown in Fig. 3(a). The optical spectrum was found to center at 1041.01 nm with the full-width at half-maximum (FWHM) of 1.59 nm. The longitudinal mode spacing was 0.080 nm which agrees with the pulse repetition rate shown in Fig. 3(a).

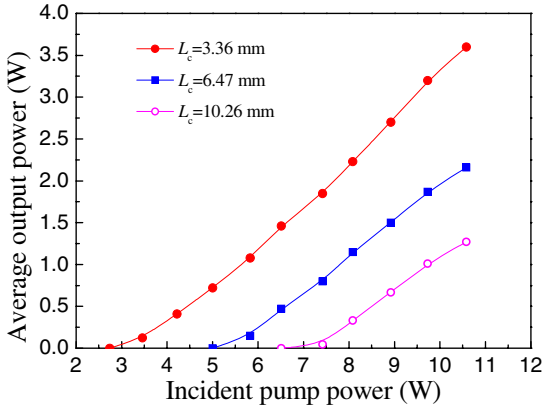

Fig. 2. Dependence of the averaged output power on the incident pump power with different optical cavity length.

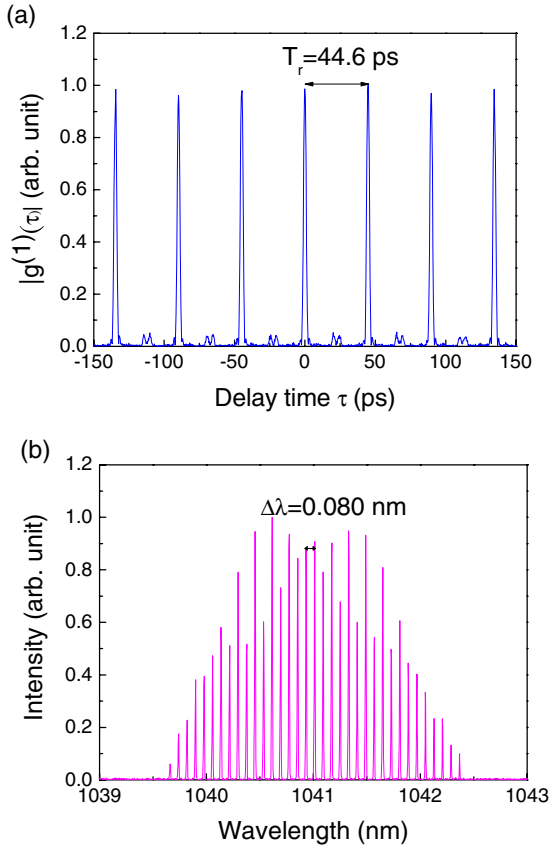

Fig. 3. (a) Experimental traces of the temporal behavior of first-order autocorrelation with the cavity length of 6.69 mm. (b) Optical spectrum corresponding to the first-order autocorrelation trace shown in (a).

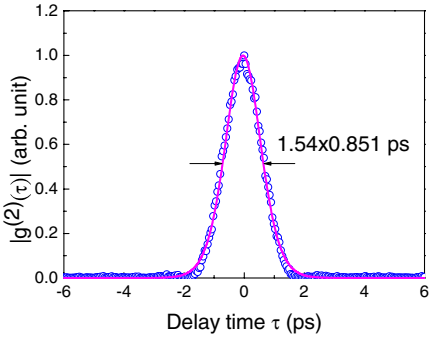

Fig. 4. FWHM width of a single pulse of the second-order autocorrelations with the cavity length of 6.69 mm.

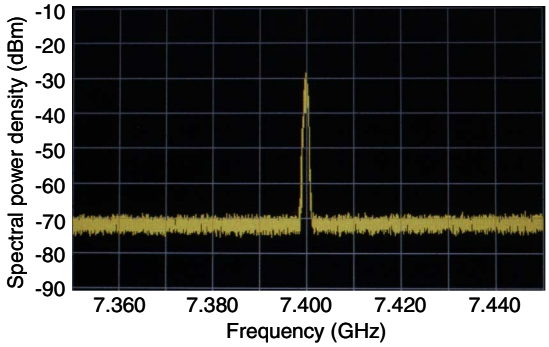

Fig. 6. RF spectrum with a resolution bandwidth of 100 kHz and a span of 100 MHz.

The FWHM width of the single pulse of the second-order autocorrelation trace is shown in Fig. 4. Assuming the sech^2-shaped temporal profile, the pulse duration was estimated to be 850 fs. Consequently, the time-bandwidth product of the mode-locked pulse is found to be 0.374 that is slightly larger than the Fourier-limited value of 0.32. The chirped pulses mainly come from the group velocity dispersion introduced by the gain medium. With dispersion compensation by prism pairs, reduction of time-bandwidth product had been demonstrated [14].

As shown in Fig. 5(a), the pulse repetition rate decreases with increasing the Yb:KGW crystal length. The repetition rates can be seen to be 22.4, 11.7, and 7.4 GHz, corresponding to the optical cavity lengths of 6.69, 12.85, and 20.38 mm, respectively. On the other hand, the center wavelength of the laser output increases with increasing crystal length. As shown in Fig. 5(a), the center wavelengths are 1041.01, 1043.42, and 1045.63 nm for the crystal lengths of 3.36, 6.47, and 10.26 mm, respectively. The wavelength shift mainly comes from the more residual absorption of the longer gain medium and the thermal excitation of the lower lasing levels [15]. The pulse durations and FWHMs of the lasing spectra versus different cavity lengths are depicted in Fig. 5(b). The reduction in the spectral bandwidth of the longer crystal arises from the increase in the strength of the re-absorption loss, due to the quasi-three-level nature of the Yb:KGW crystal. As a result, the pulse duration grows with increasing length of the gain medium from 0.85 ps for the 3.36 mm laser crystal to 1.52 ps for the 10.26 mm laser crystal. To confirm the performance of the self-mode-locked Yb:KGW laser, the RF spectrum for the cavity length of 20.38 mm that spanned of 100 MHz with 100 KHz resolution bandwidth is measured in Fig. 6. It can be seen that the signal-to-noise is greater than 40 dBm which is comparable to or better than other SML results [16,17]. The oscilloscope trace of the output pulse train with a time span of 1 μs demonstrating the amplitude stability is shown in Fig. 7. The temporal trace shows stable continuous wave mode-locking state without self-Q-switched or relaxation oscillation phenomena. Owing to the high intracavity circulating power and small area in the gain medium, the laser oscillator always operates above the Q-switching instability. To the best of our knowledge, this is the first time that a sub-ps, high-power Yb:KGW laser was realized with the SML operation at pulse repetition rate above 10 GHz.

In summary, we have employed the Yb:KGW crystal as a monolithic cavity to achieve an efficiently high-power SML operation with the repetition rate up to several tens of GHz. We explored the influence of the crystal length

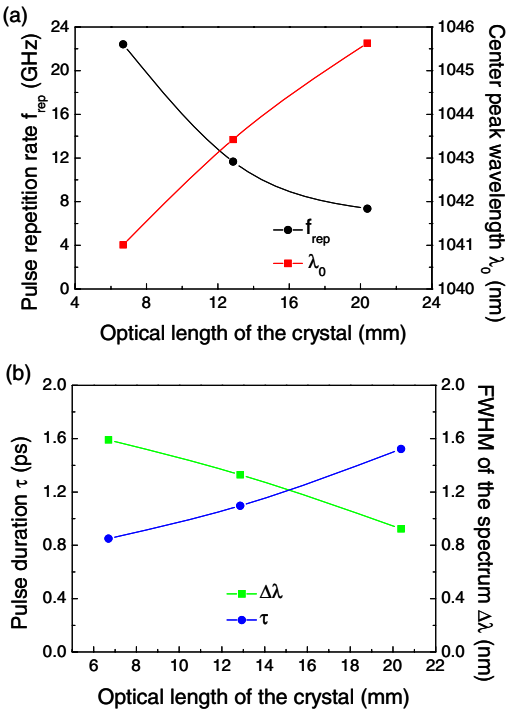

Fig. 5. (a) Pulse repetition rate and the center peak of the laser spectra obtained with different cavity lengths. (b) FWHM widths of a single pulse of the second-order autocorrelations and the output laser spectra versus diverse cavity length.

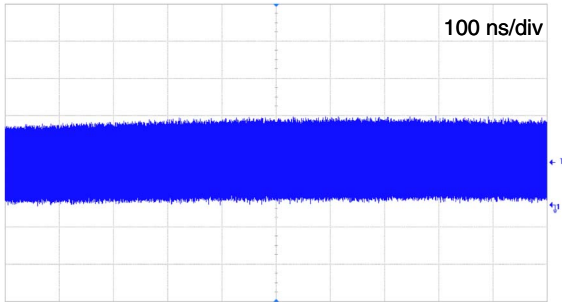

Fig. 7. Continuous wave mode-locking pulse train oscilloscope trace with time span of 1 μs.

on the average output power, the pulse repetition rate, and the pulse duration. With a crystal length of 3.36 mm, we have obtained the mode-locked pulse with duration of 850 fs at a repetition rate of 22.4 GHz. The average output power was up to 3.6 W under the pump power of 10.5 W, which corresponds to the optical efficiency of 34.3%. This sub-ps, high-power Yb:KGW laser with ultra-high repetition rate is expected to be a useful light source for many applications.

The authors thank the National Science Council of Taiwan for their financial support of this research under Contract No. NSC-100-2628-M-009-001-MY3.

References

1. V. Gerginov, C. E. Tanner, S. A. Diddams, A. Bartels, and L. Hollberg, Opt. Lett. **30**, 1734 (2005).
2. H. Hu, H. C. H. Mulvad, C. Peucheret, M. Galili, A. Clausen, P. Jeppesen, and L. K. Oxenløwe, Opt. Express **19**, B343 (2011).
3. D. Kielpinski, Phys. Rev. A **73**, 063407 (2006).
4. Y. Sun, J. Q. Pan, L. J. Zhao, W. Chen, W. Wang, L. Wang, X. F. Zhao, and C. Y. Lou, IEEE J. Lightwave Technol. **28**, 2521 (2010).
5. S. T. Cundiff and A. M. Weiner, Nat. Photonics **4**, 760 (2010).
6. Y. F. Chen, W. Z. Zhuang, H. C. Liang, G. W. Huang, and K. W. Su, Laser Phys. Lett. **10**, 1 (2012).
7. G. Q. Xie, D. Y. Tang, L. M. Zhao, L. J. Qian, and K. Ueda, Opt. Lett. **32**, 2741 (2007).
8. A. A. Lagatsky, C. T. A. Brown, and W. Sibbett, Opt. Express **12**, 3928 (2004).
9. S. Pekarek, A. Klenner, T. Südmeyer, C. Fiebig, K. Paschke, G. Erbert, and U. Keller, Opt. Express **20**, 4248 (2012).
10. M. Endo, A. Ozawa, and Y. Kobayashi, Opt. Express **20**, 12191 (2012).
11. H. C. Liang, Y. J. Huang, W. C. Huang, K. W. Su, and Y. F. Chen, Opt. Lett. **35**, 4 (2010).
12. Y. J. Huang, Y. S. Tzeng, C. Y. Tang, Y. P. Huang, and Y. F. Chen, Opt. Express **20**, 18230 (2012).
13. A. Major, I. Nikolakakos, J. S. Aitchison, A. I. Ferguson, N. Landford, and P. W. E. Smith, Appl. Phys. B **77**, 433 (2003).
14. J. Liu, J. M. Yang, W. W. Wang, L. H. Zheng, L. B. Su, and J. Xu, Laser Phys. **21**, 659 (2011).
15. S. Uemura and K. Torizuka, in *Advanced Solid-State Photonics*, OSA Technical Digest Series (CD) (Optical Society of America, 2008), paper MC36.
16. H. C. Liang, H. L. Chang, W. C. Huang, K. W. Su, Y. F. Chen, and Y. T. Chen, Appl. Phys. B **97**, 451 (2009).
17. Y. J. Huang, H. C. Liang, Y. F. Chen, H. J. Zhang, J. Y. Wang, and M. H. Jiang, Laser Phys. **21**, 1750 (2011).